

Study of Multiphoton Final States and Tests of QED in e^+e^- collisions at \sqrt{s} up to 209 GeV

The L3 Collaboration

Abstract

The process $e^+e^- \rightarrow n\gamma$ with $n \geq 2$ is studied at centre-of-mass energies ranging from $\sqrt{s} = 192$ to 209 GeV. The data sample corresponds to a total integrated luminosity of 427 pb^{-1} . The total and differential cross sections are found to be in agreement with the QED expectations. Using all the data collected with the L3 detector above the Z pole, limits on deviations from QED, excited electrons, contact interactions, extra space dimensions and excited spin-3/2 leptons are set.

Submitted to *Phys. Lett. B*

Introduction

The process $e^+e^- \rightarrow \gamma\gamma$ receives its main contribution from QED by means of the exchange of an electron via *t*-channel. The lowest order contribution to the cross section is:

$$\left(\frac{d\sigma}{d\Omega}\right)_{QED} = \frac{\alpha^2}{s} \frac{(1 + \cos^2 \theta)}{(1 - \cos^2 \theta)}, \quad (1)$$

where θ is the polar angle of the photon, α the electromagnetic coupling constant and \sqrt{s} the centre-of-mass energy of the collision.

The experimental signature of the final state is clean, allowing the analysis of event samples with negligible background. The sensitivity of this process to deviations with respect to the QED predictions grows with \sqrt{s} and, in addition, non-QED contributions are small. Any deviation can be therefore interpreted as a sign of new physics.

In this letter, results of the study of the process $e^+e^- \rightarrow n\gamma$ ($n \geq 2$) are presented. The analysis is performed on the data collected by the L3 detector [1] at centre-of-mass energies from 191.6 to 209.2 GeV, for a total integrated luminosity of 427 pb^{-1} . The luminosities as a function of \sqrt{s} are detailed in Table 1. L3 results at $\sqrt{s} = 91 - 189$ GeV [2–5] are included in the interpretations. Similar studies at \sqrt{s} up to 202 GeV were reported by other experiments [6].

Event Selection

The event selection proceeds from photon candidates, defined as:

- A shower in the electromagnetic calorimeter with an energy above 5 GeV having a profile consistent with that of a photon or an electron.
- The number of hits in the vertex chamber within an azimuthal angle of $\pm 8^\circ$ around the path of the photon candidate must be less than the 40% of that expected for a charged particle.

There must be at least two photon candidates with polar angles θ_γ between 16° and 164° , for the shower to be fully contained in the electromagnetic calorimeter and to ensure a sufficient number of hits in the vertex chamber in order to reject electrons. The angular separation between the two photons must be more than 15° . In addition, to reject $e^+e^- \rightarrow \nu\bar{\nu}\gamma\gamma$ and cosmic ray, events the sum of the energies of the photon candidates is required to be larger than $\sqrt{s}/2$. Events containing any track with momentum larger than 0.1 GeV pointing in a cone of 2.5° around any additional calorimetric cluster are rejected. A scintillator signal in coincidence with the beam crossing time and associated to a photon is also required.

The background in the sample selected with these cuts, estimated from Monte Carlo simulations, is negligible. The efficiencies to detect at least two photons in the angular region $16^\circ < \theta_\gamma < 164^\circ$ are computed from a Monte Carlo generator [7] of $e^+e^- \rightarrow \gamma\gamma(\gamma)$ events of order α^3 , passed through the L3 simulation [8] and reconstruction programs. They are presented in Table 1. Trigger inefficiencies, as estimated using Bhabha events, which have an independent trigger for charged particles, are found to be negligible.

Analysis of the Sample

After the selection criteria described above, events are classified according to the number of isolated photons in the angular range $16^\circ < \theta_\gamma < 164^\circ$. Table 2 lists the number of observed and expected events. No events with four or more photons are observed while 0.3 are expected [3]. One event with four photons was observed at $\sqrt{s} = 130$ GeV [3] and another one at $\sqrt{s} = 183$ GeV [5]. Integrating in the range $\sqrt{s} = 130 - 209$ GeV, 0.7 of such events are expected. The distributions of the acollinearity, the sum of the energies of the two most energetic photons and the polar angles of the most and least energetic photons are presented in Figure 1. These distributions are obtained combining all data at $\sqrt{s} = 192 - 209$ GeV.

The total cross sections are measured from the number of observed events. They are presented in Table 3 together with the QED expectations [7]. Good agreement is observed. The uncertainty in the QED prediction, due to the missing contribution of higher order corrections, is estimated to be 1%. These measurements and the previously measured values [2–5] are presented in Figure 2 as a function of the centre-of-mass energy and compared to the QED expectations. The global χ^2 of the data with respect to the theoretical prediction is 5.8 for 12 degrees of freedom, and the average ratio between the measured cross section, σ_{measured} , and the QED predicted cross section, σ_{QED} , is: $\sigma_{\text{measured}}/\sigma_{\text{QED}} = 0.986 \pm 0.012 \pm 0.010$, where the first uncertainty is experimental and the second theoretical.

The statistical uncertainty dominates the measurements. The main systematic source is the efficiency of the selection procedure. It is evaluated varying the selection criteria and taking into account the finite Monte Carlo statistics. The systematic effects due to the uncertainties in the measured luminosity and to the residual background are found to be negligible.

The differential cross sections as a function of the polar angle are computed. The event polar angle, $\cos \theta$, is defined as $\cos \theta = |\sin(\frac{\theta_1-\theta_2}{2})/\sin(\frac{\theta_1+\theta_2}{2})|$, where θ_1 and θ_2 are the polar angles of the two most energetic photons in the event. They are compared with the lowest order QED predictions for each \sqrt{s} in Figure 3. A finer binning is presented in Table 4. The table includes the bin-by-bin efficiencies and the multiplicative factors used to bring the cross section to the lowest order.

The agreement between data and expectations allows to constrain new physics models. They are discussed in what follows.

Limits on Deviations from QED

The possible deviations from QED are parametrised in terms of effective Lagrangians. Their effect on the observables is expressed as a multiplicative correction term to the QED differential cross-section. Depending on the type of parametrisation two general forms are considered [9]:

$$\frac{d\sigma}{d\Omega} = \left(\frac{d\sigma}{d\Omega} \right)_{\text{QED}} \left(1 + \frac{s^2}{\alpha} \frac{1}{\Lambda^4} \sin^2 \theta \right) \quad (2)$$

and

$$\frac{d\sigma}{d\Omega} = \left(\frac{d\sigma}{d\Omega} \right)_{\text{QED}} \left(1 + \frac{s^3}{32\pi\alpha^2} \frac{1}{\Lambda'^6} \frac{\sin^2 \theta}{1 + \cos^2 \theta} \right), \quad (3)$$

which depend on the centre-of-mass energy, the polar angle θ and the scale parameters Λ or Λ' . A simple and convenient way of parametrising the deviations from QED is the introduction

of the cut-off parameters Λ_{\pm} [10]. The differential cross-section in this case is obtained from Equation 2 replacing Λ^4 by $\pm(2/\alpha)\Lambda_{\pm}^4$. The effects of deviations of this type on the differential cross section are presented in Figure 4.

Combining the present results with those obtained in our previous analyses [3–5], the estimated parameters are:

$$\begin{aligned}\frac{1}{\Lambda^4} &= (-0.01^{+0.03}_{-0.02}) \times 10^{-11} \text{ GeV}^{-4}, \\ \frac{1}{\Lambda'^6} &= (-0.03^{+0.06}_{-0.04}) \times 10^{-16} \text{ GeV}^{-6}.\end{aligned}$$

Normalising the corresponding probability density function over the physically allowed range of the parameters, the following limits at the 95% confidence level (CL) are obtained:

$$\begin{aligned}\Lambda &> 1.6 \text{ TeV}, \\ \Lambda_+ &> 0.4 \text{ TeV}, \\ \Lambda_- &> 0.3 \text{ TeV}, \\ \Lambda' &> 0.8 \text{ TeV}.\end{aligned}$$

Search for Excited Electrons

Another way to study possible deviations from QED is to postulate the existence of an excited electron e^* of mass m_{e^*} , which couples to the electron and the photon via chiral magnetic interactions. This coupling is described by the phenomenological Lagrangian [11]:

$$\mathcal{L} = \frac{e}{2\Lambda_{e^*}} \bar{\Psi}_{e^*} \sigma^{\mu\nu} (1 \pm \gamma^5) \Psi_e F_{\mu\nu} + h.c. \quad (4)$$

The parameter Λ_{e^*} is related to the effective scale of the interaction. The effect on the differential cross section due to the presence of an excited electron with $\Lambda_{e^*} = m_{e^*}$ is depicted in Figure 4. From a fit to the data, we obtain:

$$\frac{1}{\Lambda_{e^*}^4} = (-0.09^{+0.20}_{-0.17}) \times 10^{-9} \text{ GeV}^{-4}.$$

Fixing the interaction scale Λ_{e^*} to m_{e^*} , we derive a 95% CL lower limit of:

$$m_{e^*} > 0.31 \text{ TeV}.$$

No excited electron mass limit with a purely magnetic interaction [12] is given, since the limits derived from $g_e - 2$ measurements already exclude [13] the scales accessible at LEP.

Low Scale Gravity Effects

The differential cross section for photon pair production in e^+e^- collisions is modified in the presence of Low Scale Gravity and extra space dimensions [14,15]. From Reference 15 it follows:

$$\frac{d\sigma}{d\Omega} = \left(\frac{d\sigma}{d\Omega} \right)_{QED} \left(1 - \frac{\lambda s^2}{2\pi\alpha M_S^4} (1 - \cos^2\theta) + \frac{\lambda^2 s^4}{16\pi^2\alpha^2 M_S^8} (1 - \cos^2\theta)^2 \right). \quad (5)$$

The deviations are weighted by a factor λ which absorbs the full dependence on the details of the theory. The parameter $\lambda = \pm 1$ is chosen to allow for the different signs of the interference. The pure gravitational part in the third term never exceeds 1% of the second term, the interference one, and is thus neglected. From a comparison of Equations 2 and 5 it follows:

$$-\frac{\lambda}{M_S^4} = \pm \frac{\pi\alpha}{\Lambda_\pm^4}.$$

The modified differential cross section is shown in Figure 4. Lower limits at 95% CL on the value of the scale M_S , derived from the limits on Λ_\pm , are:

$$\begin{aligned} M_S(\lambda = +1) &> 0.84 \text{ TeV}, \\ M_S(\lambda = -1) &> 0.99 \text{ TeV}. \end{aligned}$$

Search for Excited Spin-3/2 Leptons

Supersymmetry and composite models [16] predict the existence of spin-3/2 particles, and $e^+e^- \rightarrow \gamma\gamma$ production is a suitable process to search for their effect. Field theories for spin-3/2 particles are known to be non-renormalizable, but two effective interaction Lagrangians [17], with vector or tensor interactions, can be used to describe this contribution:

$$\begin{aligned} \mathcal{L}_{int}^{(1)} &= \frac{e}{M_{3/2,V}} \bar{\Psi}_\mu^* \gamma_\nu (c_L \psi_L + c_R \psi_R) F^{\mu\nu}, \\ \mathcal{L}_{int}^{(2)} &= \frac{e}{M_{3/2,T}^2} \bar{\Psi}_\mu^* \sigma_{\alpha\beta} (c_L \psi_L + c_R \psi_R) \partial^\mu F^{\alpha\beta}, \end{aligned} \quad (6)$$

where Ψ_μ refers to the spin-3/2 lepton, ψ_L and ψ_R are the left and right handed electron fields, respectively, c_L and c_R are the corresponding coupling strengths, and $F^{\mu\nu}$ the electromagnetic field tensor. The parameters $M_{3/2,i}$ ($i = V, T$) are the masses of the excited lepton for each hypothesis, and are also identified with the scale of new physics. The presence of such lepton modifies the differential cross section of the $e^+e^- \rightarrow \gamma\gamma$ process as presented in Figure 4.

A search for excited spin-3/2 leptons is performed using all data collected with L3 above the Z pole under the assumption $c_R = 0$. Deviations from QED are invariant under the interchange between c_L and c_R [17]. Figure 5 presents the 95% CL excluded regions in the $(c_L^2, M_{3/2,i})$ planes. The 95% CL limits obtained for $c_L^2 = 1$ are:

$$\begin{aligned} M_{3/2,V} &> 0.19 \text{ TeV}, \\ M_{3/2,T} &> 0.20 \text{ TeV}. \end{aligned}$$

References

- [1] L3 Collaboration, B. Adeva *et al.*, Nucl. Instr. and Meth. **A 289** (1990) 35;
M. Chemarin *et al.*, Nucl. Instr. and Meth. **A 349** (1994) 345;
M. Acciarri *et al.*, Nucl. Instr. and Meth. **A 351** (1994) 300;
G. Basti *et al.*, Nucl. Instr. and Meth. **A 374** (1996) 293;
I.C. Brock *et al.*, Nucl. Instr. and Meth. **A 381** (1996) 236;
A. Adam *et al.*, Nucl. Instr. and Meth. **A 383** (1996) 342.
- [2] L3 Collaboration, M. Acciarri *et al.*, Phys. Lett. **B 353** (1995) 136.
- [3] L3 Collaboration, M. Acciarri *et al.*, Phys. Lett. **B 384** (1996) 323.
- [4] L3 Collaboration, M. Acciarri *et al.*, Phys. Lett. **B 413** (1997) 159.
- [5] L3 Collaboration, M. Acciarri *et al.*, Phys. Lett. **B 475** (2000) 198.
- [6] ALEPH Collaboration, D. Buskulic *et al.*, Phys. Lett. **B 429** (1998) 201.
DELPHI Collaboration, P. Abreu *et al.*, Phys. Lett. **B 491** (2000) 67.
OPAL Collaboration, K. Ackerstaff *et al.*, Phys. Lett. **B 465** (1999) 303.
- [7] F. A. Berends and R. Kleiss, Nucl. Phys. **B 186** (1981) 22;
CALKUL Collaboration, F. A. Berends *et al.*, Nucl. Phys. **B 239** (1984) 395.
- [8] The L3 detector simulation is based on GEANT Version 3.15,
R. Brun *et al.*, Preprint CERN DD/EE/84-1 (1987), revised 1987;
The GHEISHA program (H. Fesefeldt, RWTH Aachen Report PITHA 85/02 (1985)) is used to simulate hadronic interactions.
- [9] O. J. P. Eboli *et al.*, Phys. Lett. **B 271** (1991) 274.
- [10] R. P. Feynman, Phys. Rev. Lett. **74** (1948) 939;
S. Drell, Ann. Phys. (N.Y.) **4** (1958) 75;
F.E. Low, Phys. Rev. Lett. **14** (1965) 238;
F. M. Renard, Phys. Lett. **B 116** (1982) 264.
- [11] K. Hagiwara, S. Komamyia and D. Zeppenfeld, Z. Phys. **C 29** (1985) 115;
N. Cabibbo, L. Maiani and Y. Srivastava, Phys. Lett **B 139** (1984) 459;
F.M. Renard, Nucl. Phys. **B 196** (1982) 93.
- [12] A. Litke, Harvard Univ., Ph.D Thesis (1970) unpublished.
- [13] F. M. Renard, Phys. Lett. **B 116** (1982) 264.
- [14] G. F. Giudice *et al.*, Nucl. Phys. **B 544** (1999) 3.
- [15] K. Agashe and N. G. Deshpande, Phys. Lett. **B 456** (1999) 60.
- [16] J. Kühn and P. Zerwas, Phys. Lett. **B 147** (1984) 189;
S. R. Choudhury, R. G. Ellis and G. C. Joshi, Phys. Rev. **D 31** (1985) 2390.
- [17] R. Walsh and A. J. Ramalho, Phys. Rev. **D 60** (1999) 077302.

The L3 Collaboration:

P.Achard,²⁰ O.Adriam,¹⁷ M.Aguilar-Benitez,²⁴ J.Alcaraz,^{24,18} G.Alemanni,²² J.Allaby,¹⁸ A.Aloisio,²⁸ M.G.Alvaggi,²⁸ H.Anderhub,⁴⁶ V.P.Andreev,^{6,33} F.Anselmo,⁹ A.Arefiev,²⁷ T.Azemoon,³ T.Aziz,^{10,18} P.Bagnaia,³⁸ A.Bajo,²⁴ G.Baksay,¹⁶ L.Baksay,²⁵ S.V.Baldew,² S.Banerjee,¹⁰ Sw.Banerjee,⁴ A.Barczyk,^{46,44} R.Barillère,¹⁸ P.Bartalini,²² M.Basile,⁹ N.Batalova,⁴³ R.Battiston,³² A.Bay,²² F.Becattini,¹⁷ U.Becker,¹⁴ F.Behner,⁴⁶ L.Bellucci,¹⁷ R.Berbeco,³ J.Berdugo,²⁴ P.Berges,¹⁴ B.Bertucci,³² B.L.Betev,⁴⁶ M.Biasini,³² M.Biglietti,²⁸ A.Biland,⁴⁶ J.J.Blaising,⁴ S.C.Blyth,³⁴ G.J.Bobbink,² A.Böhm,¹ L.Boldizsar,¹³ B.Borgia,³⁸ S.Bottai,¹⁷ D.Bourilkov,⁴⁶ M.Bourquin,²⁰ S.Braccini,²⁰ J.G.Branson,⁴⁰ F.Brochu,⁴ J.D.Burger,¹⁴ W.J.Burger,³² X.D.Cai,¹⁴ M.Capell,¹⁴ G.Cara Romeo,⁹ G.Carlino,²⁸ A.Cartacci,¹⁷ J.Casaus,²⁴ F.Cavallari,³⁸ N.Cavallo,³⁵ C.Cecchi,³² M.Cerrada,²⁴ M.Chamizo,²⁰ Y.H.Chang,⁴⁸ M.Chemarin,²³ A.Chen,⁴⁸ G.Chen,⁷ G.M.Chen,⁷ H.F.Chen,²¹ H.S.Chen,⁷ G.Chiefari,²⁸ L.Cifarelli,³⁹ F.Cindolo,⁹ I.Clare,¹⁴ R.Clare,³⁷ G.Coignet,⁴ N.Colino,²⁴ S.Costantini,³⁸ B.de la Cruz,²⁴ S.Cucciarelli,³² J.A.van Dalen,³⁰ R.de Asmundis,²⁸ P.Déglon,²⁰ J.Debreczeni,¹³ A.Degré,⁴ K.Deiters,⁴⁴ D.della Volpe,²⁸ E.Delmeire,²⁰ P.Denes,³⁶ F.DeNotaristefani,³⁸ A.De Salvo,⁴⁶ M.Diemoz,³⁸ M.Dierckxsens,² C.Dionisi,³⁸ M.Dittmar,^{46,18} A.Doria,²⁸ M.T.Dova,^{11,‡} D.Duchesneau,⁴ B.Echenard,²⁰ A.Eline,¹⁸ H.El Mamouni,²³ A.Engler,³⁴ F.J.Eppeling,¹⁴ A.Ewers,¹ P.Extermann,²⁰ M.A.Falagan,²⁴ S.Falciano,³⁸ A.Favara,³¹ J.Fay,²³ O.Fedin,³³ M.Felcini,⁴⁶ T.Ferguson,³⁴ H.Fesefeldt,¹ E.Fiandrini,³² J.H.Field,²⁰ F.Filthaut,³⁰ P.H.Fisher,¹⁴ W.Fisher,³⁶ I.Fisk,⁴⁰ G.Forconi,¹⁴ K.Freudenreich,⁴⁶ C.Fureta,²⁶ Yu.Galaktionov,^{27,14} S.N.Ganguli,¹⁰ P.Garcia-Abia,^{5,18} M.Gataullin,³¹ S.Gentile,³⁸ S.Giagu,³⁸ Z.F.Gong,²¹ G.Grenier,²³ O.Grimm,⁴⁶ M.W.Gruenewald,^{8,1} M.Guida,³⁹ R.van Gulik,² V.K.Gupta,³⁶ A.Gurtu,¹⁰ L.J.Gutay,⁴³ D.Haas,⁵ D.Hatzifotiadou,⁹ T.Hebbeker,^{8,1} A.Hervé,¹⁸ J.Hirschfelder,³⁴ H.Hofer,⁴⁶ M.Hohlmann,²⁵ G.Holzner,⁴⁶ S.R.Hou,⁴⁸ Y.Hu,³⁰ B.N.Jin,⁷ L.W.Jones,³ P.de Jong,² I.Josa-Mutuberria,²⁴ D.Käfer,¹ M.Kaur,¹⁵ M.N.Kienzle-Focacci,²⁰ J.K.Kim,⁴² J.Kirkby,¹⁸ W.Kittel,³⁰ A.Klimentov,^{14,27} A.C.König,³⁰ M.Kopal,⁴³ V.Koutsenko,^{14,27} M.Kräber,⁴⁶ R.W.Kraemer,³⁴ W.Krenz,¹ A.Krüger,⁴⁵ A.Kunin,¹⁴ P.Ladron de Guevara,²⁴ I.Laktineh,²³ G.Landi,¹⁷ M.Lebeau,¹⁸ A.Lebedev,¹⁴ P.Lebrun,²³ P.Lecomte,⁴⁶ P.Lecoq,¹⁸ P.Le Coultre,⁴⁶ J.M.Le Goff,¹⁸ R.Leiste,⁴⁵ P.Levtchenko,³³ C.Li,²¹ S.Likhoded,⁴⁵ C.H.Lin,⁴⁸ W.T.Lin,⁴⁸ F.L.Linde,² L.Lista,²⁸ Z.A.Liu,⁷ W.Lohmann,⁴⁵ E.Longo,³⁸ Y.S.Lu,⁷ K.Lübelsmeyer,¹ C.Luci,³⁸ L.Luminari,³⁸ W.Lustermann,⁴⁶ W.G.Ma,²¹ L.Malgeri,²⁰ A.Malinin,²⁷ C.Maňa,²⁴ D.Mangeol,³⁰ J.Mans,³⁶ J.P.Martin,²³ F.Marzano,³⁸ K.Mazumdar,¹⁰ R.R.McNeil,⁶ S.Mele,^{18,28} L.Merola,²⁸ M.Meschini,¹⁷ W.J.Metzger,³⁰ A.Mihul,¹² H.Milcent,¹⁸ G.Mirabelli,³⁸ J.Mnich,¹ G.B.Mohanty,¹⁰ G.S.Muanza,²³ A.J.M.Muijs,² B.Musicar,⁴⁰ M.Musy,³⁸ S.Nagy,¹⁶ S.Natale,²⁰ M.Napolitano,²⁸ F.Nessi-Tedaldi,⁴⁶ H.Newman,³¹ T.Niessen,¹ A.Nisati,³⁸ H.Nowak,⁴⁵ R.Ofierzynski,⁴⁶ G.Organtini,³⁸ C.Palomares,¹⁸ D.Pandoulas,¹ P.Paolucci,²⁸ R.Paramatti,³⁸ G.Passaleva,¹⁷ S.Patricelli,²⁸ T.Paul,¹¹ M.Pauluzzi,³² C.Paus,¹⁴ F.Pauss,⁴⁶ M.Pedace,³⁸ S.Pensotti,²⁶ D.Perret-Gallix,⁴ B.Petersen,³⁰ D.Piccolo,²⁸ F.Pierella,⁹ M.Pioppi,³² P.A.Piroué,³⁶ E.Pistolesi,²⁶ V.Plyaskin,²⁷ M.Pohl,²⁰ V.Pojidaev,¹⁷ J.Pothier,¹⁸ D.O.Prokofiev,⁴³ D.Prokofiev,³³ J.Quartieri,³⁹ G.Rahal-Calot,⁴⁶ M.A.Rahaman,¹⁰ P.Raics,¹⁶ N.Raja,¹⁰ R.Ramelli,⁴⁶ P.G.Rancoita,²⁶ R.Ranieri,¹⁷ A.Raspereza,⁴⁵ P.Razis,²⁹ D.Ren,⁴⁶ M.Rescigno,³⁸ S.Reucroft,¹¹ S.Riemann,⁴⁵ K.Riles,³ B.P.Roe,³ L.Romero,²⁴ A.Rosca,⁸ S.Rosier-Lees,⁴ S.Roth,¹ C.Rosenbleck,¹ B.Roux,³⁰ J.A.Rubio,¹⁸ G.Ruggiero,¹⁷ H.Rykaczewski,⁴⁶ A.Sakharov,⁴⁶ S.Saremi,⁶ S.Sarkar,³⁸ J.Salicio,¹⁸ E.Sánchez,²⁴ M.P.Sanders,³⁰ C.Schäfer,¹⁸ V.Schegelsky,³³ S.Schmidt-Kærst,¹ D.Schmitz,¹ H.Schopper,⁴⁷ D.J.Schotanus,³⁰ G.Schowering,¹ C.Sciacca,²⁸ L.Servoli,³² S.Shevchenko,³¹ N.Shivarov,⁴¹ V.Shoutko,¹⁴ E.Shumilov,²⁷ A.Shvorob,³¹ T.Siedenburg,¹ D.Son,⁴² P.Spillantini,¹⁷ M.Steuer,¹⁴ D.P.Stickland,³⁶ B.Stoyanov,⁴¹ A.Straessner,¹⁸ K.Sudhakar,¹⁰ G.Sultanov,⁴¹ L.Z.Sun,²¹ S.Sushkov,⁸ H.Suter,⁴⁶ J.D.Swain,¹¹ Z.Szillas,^{25,¶} X.W.Tang,⁷ P.Tarjan,¹⁶ L.Tauscher,⁵ L.Taylor,¹¹ B.Tellili,²³ D.Teyssier,²³ C.Timmermans,³⁰ Samuel C.C.Ting,¹⁴ S.M.Ting,¹⁴ S.C.Tonwar,^{10,18} J.Tóth,¹³ C.Tully,³⁶ K.L.Tung,⁷ J.Ulbricht,⁴⁶ E.Valente,³⁸ R.T.Van de Walle,³⁰ V.Veszpremi,²⁵ G.Vesztergombi,¹³ I.Vetlitsky,²⁷ D.Vicinanza,³⁹ G.Viertel,⁴⁶ S.Villa,³⁷ M.Vivargent,⁴ S.Vlachos,⁵ I.Vodopianov,³³ H.Vogel,³⁴ H.Vogt,⁴⁵ I.Vorobiev,^{34,27} A.A.Vorobyov,³³ M.Wadhwa,⁵ W.Wallraff,¹ X.L.Wang,²¹ Z.M.Wang,²¹ M.Weber,¹ P.Wienemann,¹ H.Wilkens,³⁰ S.Wynhoff,³⁶ L.Xia,³¹ Z.Z.Xu,²¹ J.Yamamoto,³ B.Z.Yang,²¹ C.G.Yang,⁵ H.J.Yang,³ M.Yang,⁷ S.C.Yeh,⁴⁹ An.Zalite,³³ Yu.Zalite,³³ Z.P.Zhang,²¹ J.Zhao,²¹ G.Y.Zhu,⁷ R.Y.Zhu,³¹ H.L.Zhuang,⁷ A.Zichichi,^{9,18,19} G.Zilizi,^{25,¶} B.Zimmermann,⁴⁶ M.Zöller,¹

- 1 I. Physikalisches Institut, RWTH, D-52056 Aachen, FRG[§]
III. Physikalisches Institut, RWTH, D-52056 Aachen, FRG[§]
 - 2 National Institute for High Energy Physics, NIKHEF, and University of Amsterdam, NL-1009 DB Amsterdam, The Netherlands
 - 3 University of Michigan, Ann Arbor, MI 48109, USA
 - 4 Laboratoire d'Annecy-le-Vieux de Physique des Particules, LAPP, IN2P3-CNRS, BP 110, F-74941 Annecy-le-Vieux CEDEX, France
 - 5 Institute of Physics, University of Basel, CH-4056 Basel, Switzerland
 - 6 Louisiana State University, Baton Rouge, LA 70803, USA
 - 7 Institute of High Energy Physics, IHEP, 100039 Beijing, China[△]
 - 8 Humboldt University, D-10099 Berlin, FRG[§]
 - 9 University of Bologna and INFN-Sezione di Bologna, I-40126 Bologna, Italy
 - 10 Tata Institute of Fundamental Research, Mumbai (Bombay) 400 005, India
 - 11 Northeastern University, Boston, MA 02115, USA
 - 12 Institute of Atomic Physics and University of Bucharest, R-76900 Bucharest, Romania
 - 13 Central Research Institute for Physics of the Hungarian Academy of Sciences, H-1525 Budapest 114, Hungary[†]
 - 14 Massachusetts Institute of Technology, Cambridge, MA 02139, USA
 - 15 Panjab University, Chandigarh 160 014, India.
 - 16 KLTE-ATOMKI, H-4010 Debrecen, Hungary[¶]
 - 17 INFN Sezione di Firenze and University of Florence, I-50125 Florence, Italy
 - 18 European Laboratory for Particle Physics, CERN, CH-1211 Geneva 23, Switzerland
 - 19 World Laboratory, FBLJA Project, CH-1211 Geneva 23, Switzerland
 - 20 University of Geneva, CH-1211 Geneva 4, Switzerland
 - 21 Chinese University of Science and Technology, USTC, Hefei, Anhui 230 029, China[△]
 - 22 University of Lausanne, CH-1015 Lausanne, Switzerland
 - 23 Institut de Physique Nucléaire de Lyon, IN2P3-CNRS, Université Claude Bernard, F-69622 Villeurbanne, France
 - 24 Centro de Investigaciones Energéticas, Medioambientales y Tecnológicas, CIEMAT, E-28040 Madrid, Spain[♭]
 - 25 Florida Institute of Technology, Melbourne, FL 32901, USA
 - 26 INFN-Sezione di Milano, I-20133 Milan, Italy
 - 27 Institute of Theoretical and Experimental Physics, ITEP, Moscow, Russia
 - 28 INFN-Sezione di Napoli and University of Naples, I-80125 Naples, Italy
 - 29 Department of Physics, University of Cyprus, Nicosia, Cyprus
 - 30 University of Nijmegen and NIKHEF, NL-6525 ED Nijmegen, The Netherlands
 - 31 California Institute of Technology, Pasadena, CA 91125, USA
 - 32 INFN-Sezione di Perugia and Università Degli Studi di Perugia, I-06100 Perugia, Italy
 - 33 Nuclear Physics Institute, St. Petersburg, Russia
 - 34 Carnegie Mellon University, Pittsburgh, PA 15213, USA
 - 35 INFN-Sezione di Napoli and University of Potenza, I-85100 Potenza, Italy
 - 36 Princeton University, Princeton, NJ 08544, USA
 - 37 University of California, Riverside, CA 92521, USA
 - 38 INFN-Sezione di Roma and University of Rome, “La Sapienza”, I-00185 Rome, Italy
 - 39 University and INFN, Salerno, I-84100 Salerno, Italy
 - 40 University of California, San Diego, CA 92093, USA
 - 41 Bulgarian Academy of Sciences, Central Lab. of Mechatronics and Instrumentation, BU-1113 Sofia, Bulgaria
 - 42 The Center for High Energy Physics, Kyungpook National University, 702-701 Taegu, Republic of Korea
 - 43 Purdue University, West Lafayette, IN 47907, USA
 - 44 Paul Scherrer Institut, PSI, CH-5232 Villigen, Switzerland
 - 45 DESY, D-15738 Zeuthen, FRG
 - 46 Eidgenössische Technische Hochschule, ETH Zürich, CH-8093 Zürich, Switzerland
 - 47 University of Hamburg, D-22761 Hamburg, FRG
 - 48 National Central University, Chung-Li, Taiwan, China
 - 49 Department of Physics, National Tsing Hua University, Taiwan, China
- [§] Supported by the German Bundesministerium für Bildung, Wissenschaft, Forschung und Technologie
[†] Supported by the Hungarian OTKA fund under contract numbers T019181, F023259 and T024011.
[¶] Also supported by the Hungarian OTKA fund under contract number T026178.
[♭] Supported also by the Comisión Interministerial de Ciencia y Tecnología.
[#] Also supported by CONICET and Universidad Nacional de La Plata, CC 67, 1900 La Plata, Argentina.
[△] Supported by the National Natural Science Foundation of China.

\sqrt{s} (GeV)	Named as	\mathcal{L} (pb $^{-1}$)	Efficiency (%)
191.6	192	28.8	64.2 ± 0.5
195.5	196	82.4	64.8 ± 0.2
199.5	200	67.5	64.7 ± 0.2
201.7	202	35.9	64.3 ± 0.5
202.5–205.5	205	74.3	64.1 ± 0.2
205.5–209.2	207	138.1	63.6 ± 0.2

Table 1: Centre-of-mass energies, luminosities and selection efficiencies. Statistical uncertainties from the Monte Carlo sample are quoted.

\sqrt{s} (GeV)	Number of events			
	2γ		3γ	
	Observed	Expected	Observed	Expected
192	193	207	7	6
196	555	575	17	16
200	424	453	15	13
202	223	236	4	6
205	459	464	11	13
207	863	845	29	23

Table 2: Observed and expected number of events with two and three photons.

\sqrt{s} (GeV)	$\sigma_{measured}$ (pb)	$\sigma_{expected}$ (pb)
192	$10.83 \pm 0.74 \pm 0.13$	11.5 ± 0.1
196	$10.70 \pm 0.44 \pm 0.10$	11.1 ± 0.1
200	$10.05 \pm 0.46 \pm 0.10$	10.7 ± 0.1
202	$9.82 \pm 0.63 \pm 0.13$	10.5 ± 0.1
205	$9.87 \pm 0.45 \pm 0.10$	10.0 ± 0.1
207	$10.16 \pm 0.34 \pm 0.10$	9.9 ± 0.1

Table 3: Measured and expected cross sections in the angular region $16^\circ < \theta_\gamma < 164^\circ$. For the measured values, the first uncertainty is statistical and the second systematic. For the expected values the uncertainty due to the missing higher order contributions is estimated to be 1%.

Table 4: Number of events, efficiency and radiative correction factor applied to the data as a function of \sqrt{s} and of the event polar angle, $\cos \theta$. The values at $\sqrt{s} = 183$ and 189 GeV [5] are also listed. The uncertainty on the radiative correction factor ranges from 5% (first $\cos \theta$ bin) to 1% (last $\cos \theta$ bin) and is due to the finite Monte Carlo statistics.

$\cos \theta$	Data events/Efficiency[%] (\sqrt{s} in GeV)								Radiative correction factor
	183	189	192	196	200	202	205	207	
0.00–0.05	15/91.7	35/87.9	5/81.0	13/88.4	12/87.6	10/90.9	17/89.1	24/88.6	0.78
0.05–0.10	14/89.0	21/87.7	9/91.7	15/85.6	14/88.1	5/96.7	14/85.3	28/86.0	0.79
0.10–0.15	10/85.9	37/88.1	4/82.5	10/87.6	7/88.8	7/86.0	11/84.7	28/88.7	0.80
0.15–0.20	9/89.4	37/87.1	7/87.8	15/89.6	10/85.3	5/87.9	14/84.3	25/88.8	0.81
0.20–0.25	10/90.2	46/88.6	5/92.1	16/88.7	15/86.1	5/91.4	14/86.9	15/85.2	0.81
0.25–0.30	18/88.5	48/88.4	6/80.2	20/89.5	11/89.7	5/91.2	12/90.8	14/88.7	0.82
0.30–0.35	16/90.7	35/86.0	0/82.9	16/89.0	13/86.8	8/82.5	9/87.4	27/89.4	0.82
0.35–0.40	13/88.5	45/86.7	4/91.6	23/89.2	16/89.0	9/89.6	13/92.4	24/89.9	0.82
0.40–0.45	13/87.7	41/86.0	8/77.8	19/87.5	10/87.2	9/92.0	17/88.4	31/87.9	0.83
0.45–0.50	12/88.5	57/88.6	10/93.2	20/90.3	12/89.5	7/83.3	16/86.8	37/89.4	0.84
0.50–0.55	23/88.8	74/88.4	5/85.2	23/87.8	14/92.7	7/85.5	21/88.6	47/88.4	0.84
0.55–0.60	17/86.6	50/86.6	8/84.4	20/88.8	18/86.1	11/84.6	27/84.4	41/87.7	0.85
0.60–0.65	31/82.5	73/82.9	10/82.6	31/84.1	26/85.1	15/82.9	24/86.4	47/82.1	0.86
0.65–0.70	21/77.7	66/77.9	9/76.8	29/77.5	32/78.3	15/76.7	28/76.3	61/75.2	0.87
0.70–0.75	8/17.0	27/16.3	2/15.4	11/17.3	7/17.8	6/16.0	9/16.5	10/16.7	0.87
0.75–0.80	5/14.3	20/13.5	2/11.6	11/12.3	10/14.7	3/14.9	5/13.2	20/12.6	0.88
0.80–0.85	38/53.5	103/52.5	19/55.8	41/53.2	27/49.7	20/47.1	40/52.1	61/50.4	0.89
0.85–0.90	78/79.8	223/80.7	26/73.6	92/74.9	74/74.3	33/74.9	72/76.3	137/76.7	0.91
0.90–0.95	73/66.8	258/66.6	45/65.6	114/66.0	83/66.0	36/67.4	83/63.9	154/63.7	0.95
0.95–0.96	35/69.1	78/67.2	16/67.4	33/66.7	28/66.3	11/66.1	24/63.7	61/62.9	1.00

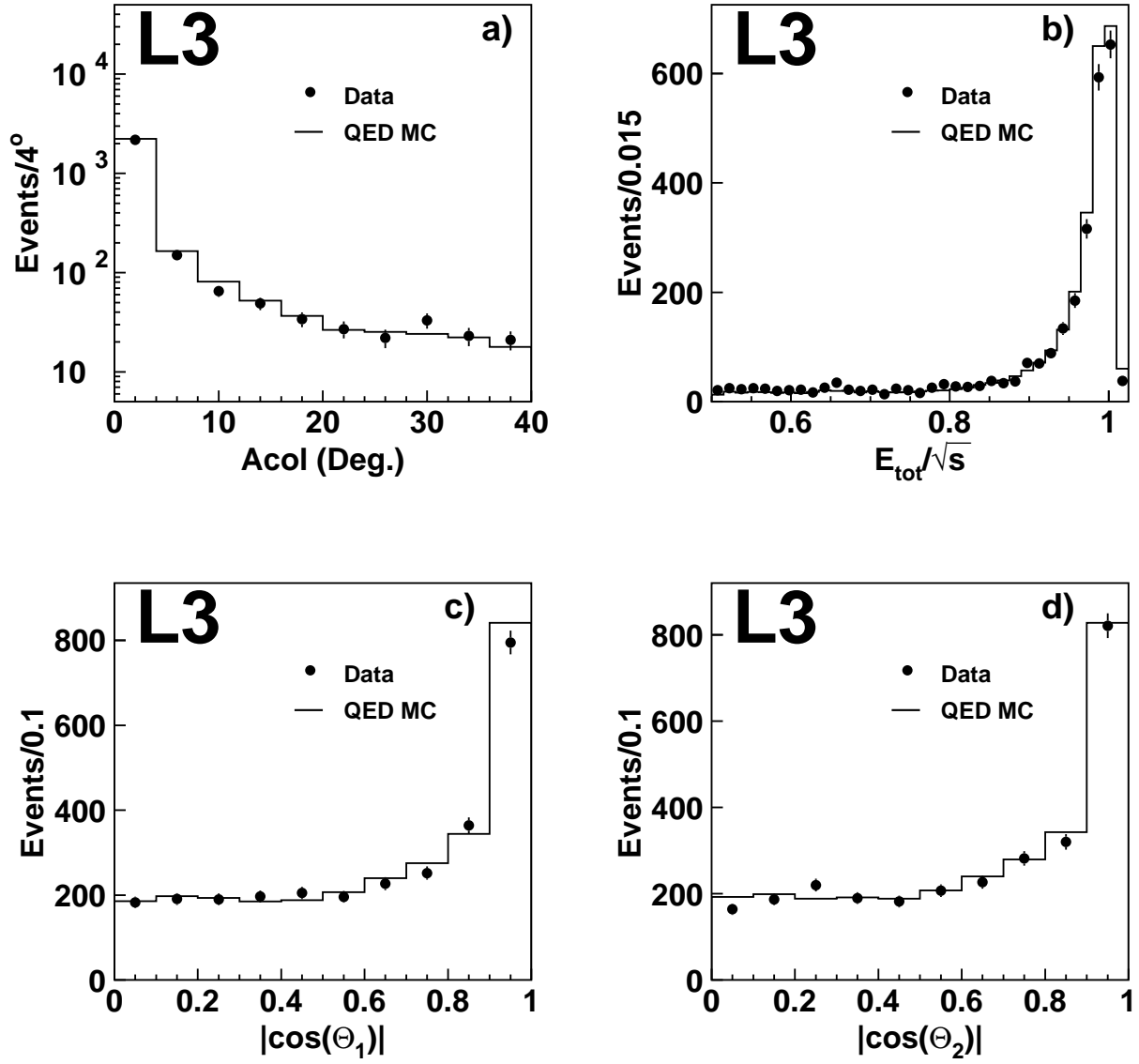


Figure 1: Distributions of a) the acollinearity angle between the two most energetic photons, b) the total energy normalized to the centre-of-mass energy and $\cos \theta$ for c) the most and d) the least energetic photon. Points are data and the histogram is the Monte Carlo prediction. The data sample collected at $\sqrt{s} = 192 - 209$ GeV is presented.

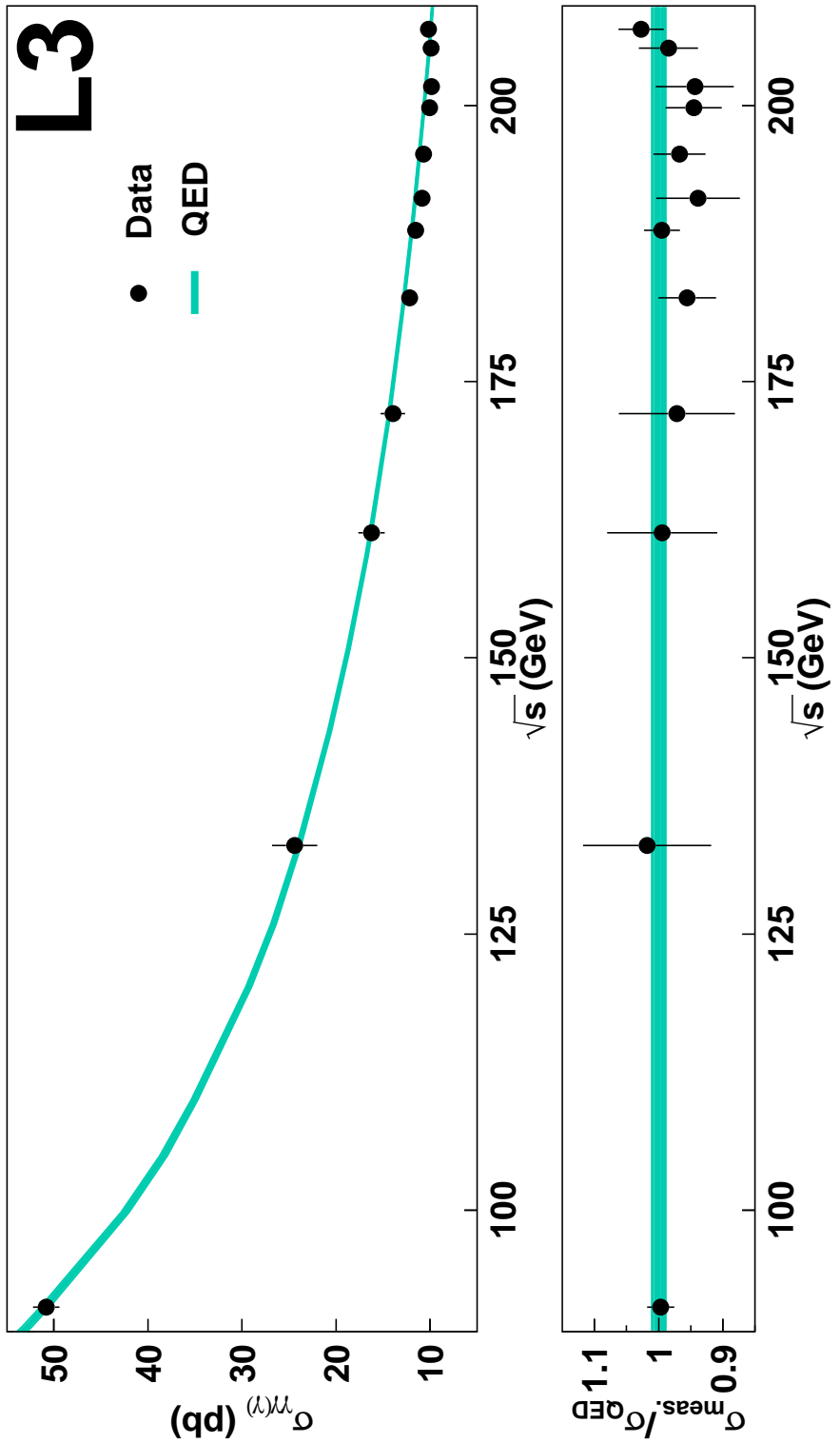


Figure 2: Measured cross sections as a function of the centre-of-mass energy in the angular region $16^\circ < \theta_\gamma < 164^\circ$, compared to QED predictions. The value at the Z pole is extrapolated to this angular range from the one given in Reference 2, resulting in a value of 50.8 ± 1.4 pb. The ratio between the measured and the expected cross sections is also presented. The line width represents the uncertainty in the QED prediction, estimated to be 1%.

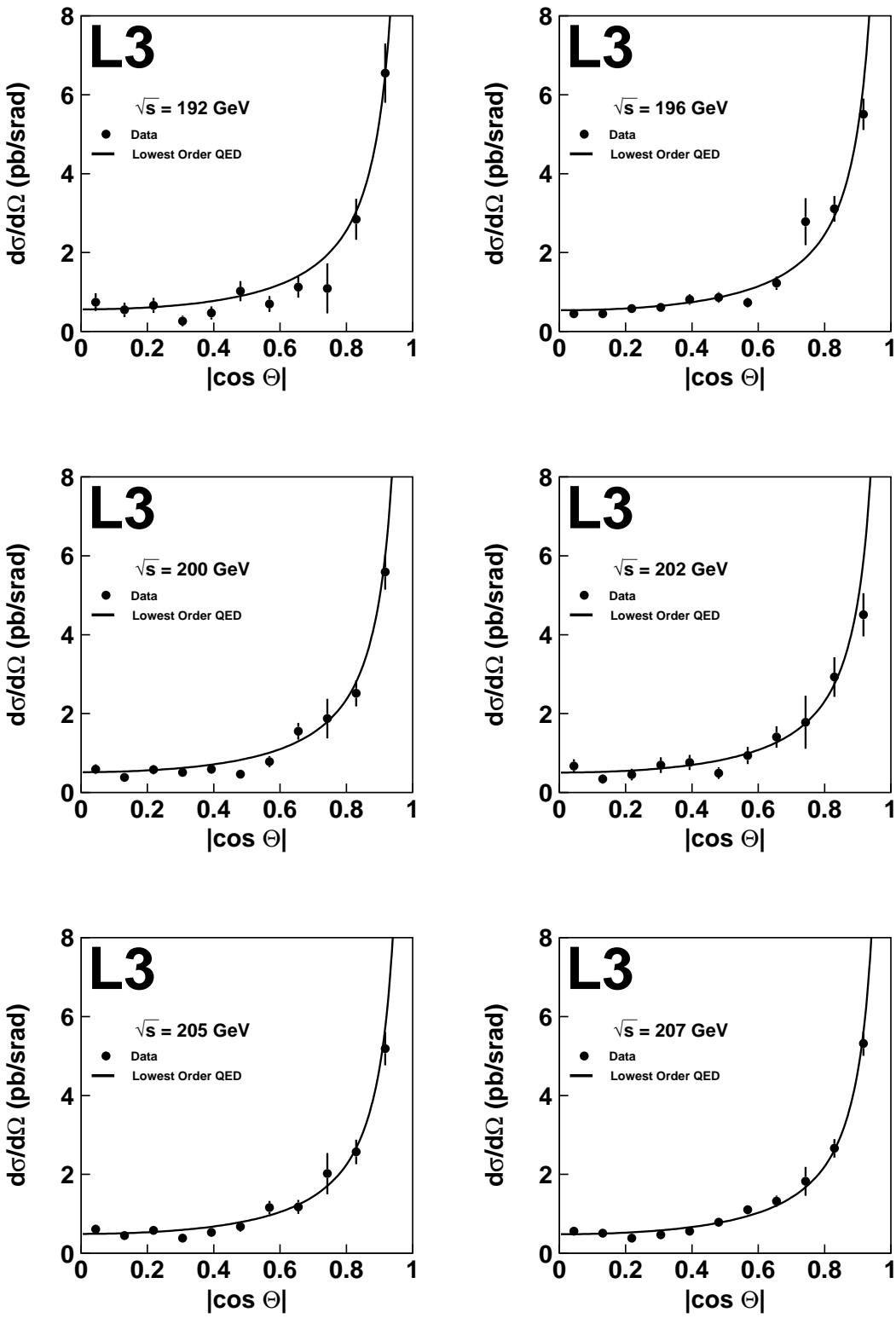


Figure 3: Differential cross sections as a function of $\cos \theta$ for different values of \sqrt{s} . Points are data and the solid line corresponds to the lowest order QED prediction.

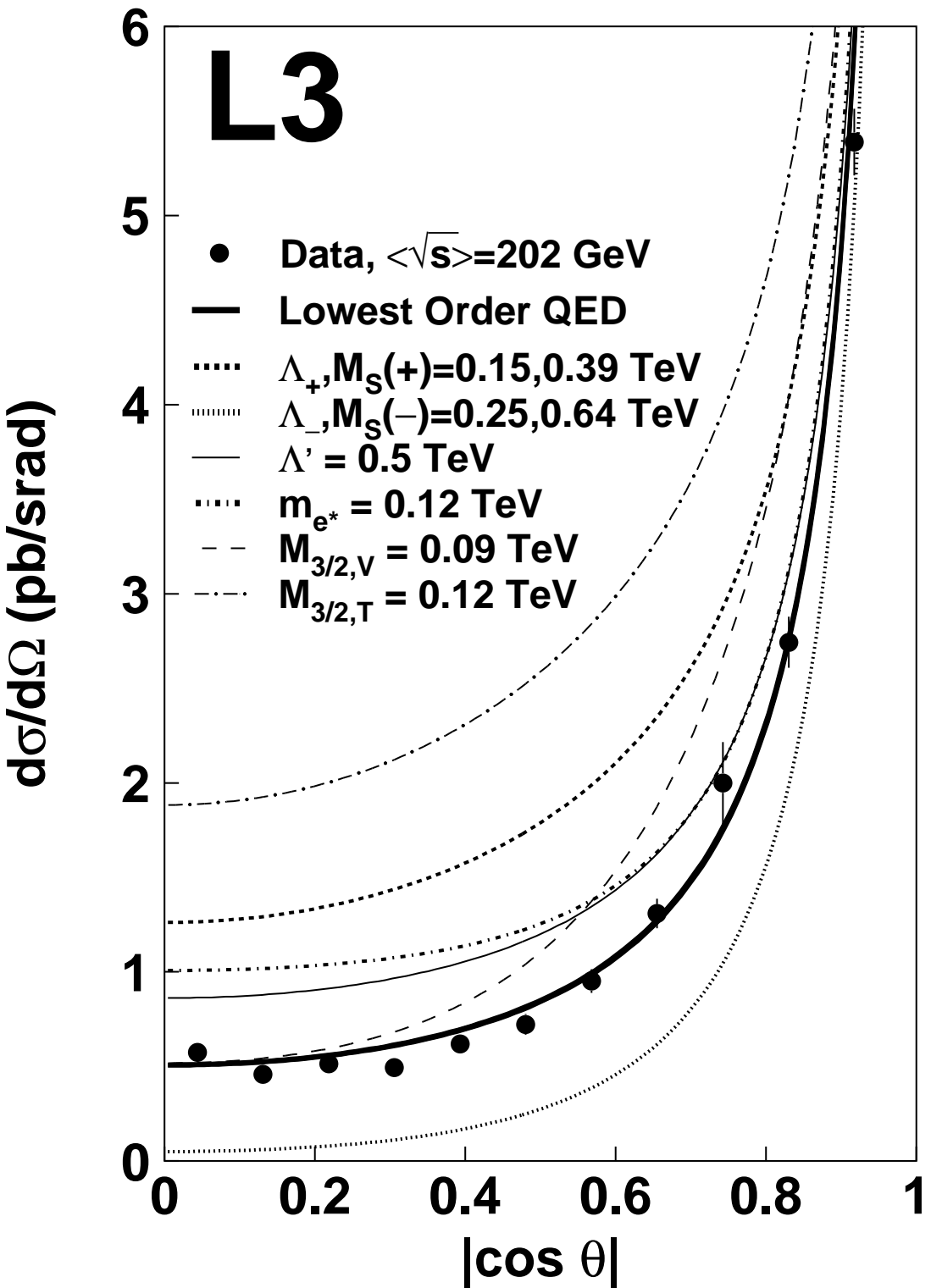


Figure 4: Differential cross sections as a function of $\cos \theta$. Points are data from $\sqrt{s} = 192$ to 208 GeV, corresponding to a luminosity weighted average of $<\sqrt{s}>= 202$ GeV. Lines show the different predictions for the models discussed in the text at a centre-of-mass energy of $<\sqrt{s}>= 202$ GeV. The width of the lowest order QED prediction takes into account the theoretical uncertainty, estimated to be 1%. The χ^2 with respect to the QED prediction is 1.6 per degree of freedom.

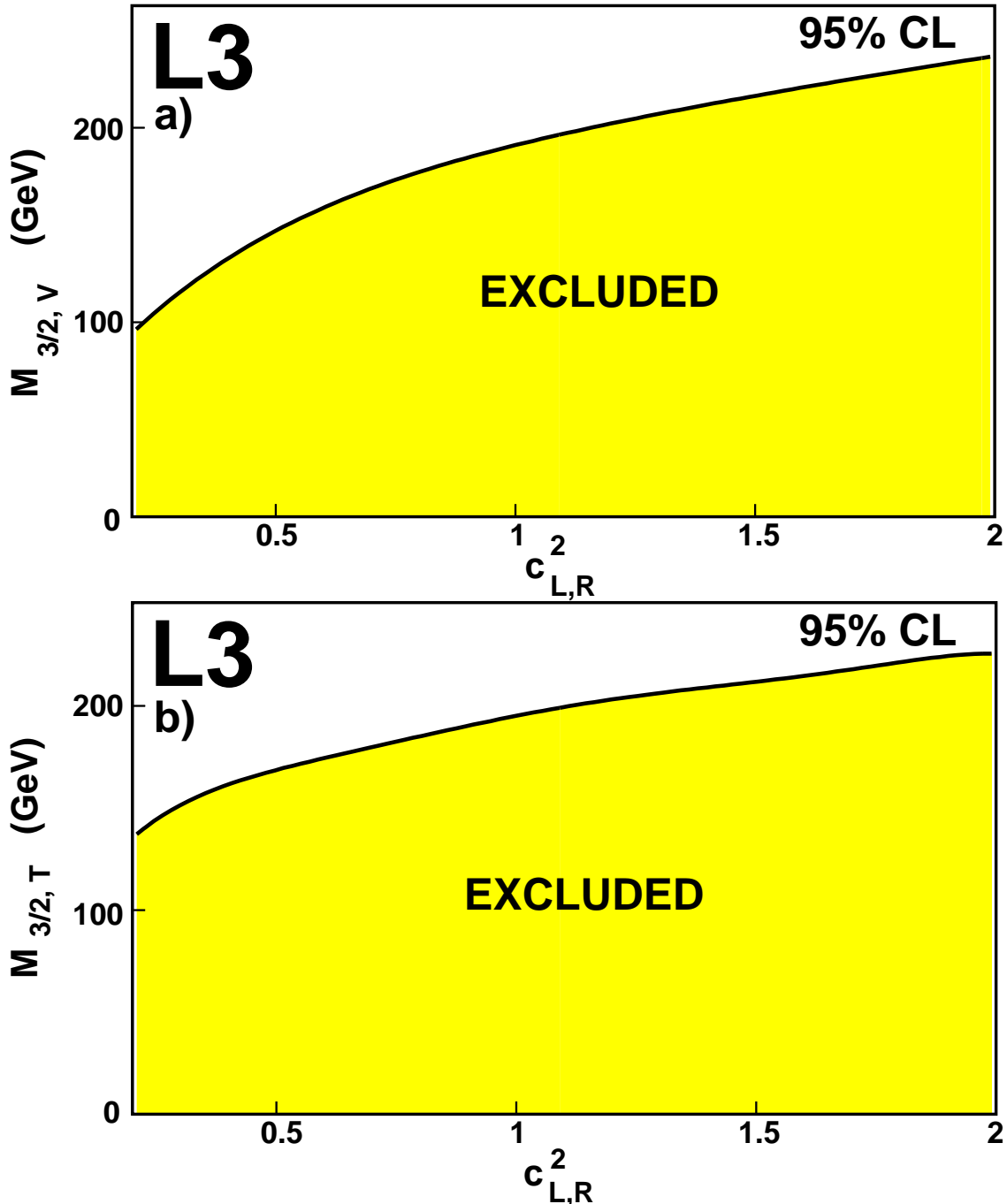


Figure 5: Excluded regions at 95% CL in the plane a) $(M_{3/2,V}^2, c_L^2)$ for the vector coupling case and b) $(M_{3/2,T}^2, c_L^2)$ for the tensor coupling hypothesis in the search for excited spin-3/2 leptons. The result is independent of the interchange between c_L and c_R [17].